



HAL
open science

Dual Beam Depth Profiling and Imaging with Argon and Bismuth Clusters of Prenylated Stilbenes on Glandular Trichomes of *Macaranga vedeliana*

Tiphaine Péresse, Nicolas Elie, David Touboul, Van-Cuong Pham, Vincent Dumontet, Fanny Roussi, Marc Litaudon, Alain Brunelle

► **To cite this version:**

Tiphaine Péresse, Nicolas Elie, David Touboul, Van-Cuong Pham, Vincent Dumontet, et al.. Dual Beam Depth Profiling and Imaging with Argon and Bismuth Clusters of Prenylated Stilbenes on Glandular Trichomes of *Macaranga vedeliana*. *Analytical Chemistry*, 2017, 89 (17), pp.9247-9252. 10.1021/acs.analchem.7b02020 . hal-03176647

HAL Id: hal-03176647

<https://hal.science/hal-03176647v1>

Submitted on 18 Aug 2022

HAL is a multi-disciplinary open access archive for the deposit and dissemination of scientific research documents, whether they are published or not. The documents may come from teaching and research institutions in France or abroad, or from public or private research centers.

L'archive ouverte pluridisciplinaire **HAL**, est destinée au dépôt et à la diffusion de documents scientifiques de niveau recherche, publiés ou non, émanant des établissements d'enseignement et de recherche français ou étrangers, des laboratoires publics ou privés.

Dual Beam Depth Profiling and Imaging with Argon and Bismuth Clusters of Prenylated Stilbenes on Glandular Trichomes of *Macaranga vedeliana*

Tiphaine Péresse,^{†,#} Nicolas Elie,^{†,#} David Touboul,[†] Van-Cuong Pham,[‡] Vincent Dumontet,[†] Fanny Roussi,[†] Marc Litaudon,[†] and Alain Brunelle^{†,*}

[†] Institut de Chimie des Substances Naturelles, CNRS UPR 2301, Univ. Paris-Sud, Université Paris-Saclay, Avenue de la Terrasse, 91198 Gif-sur-Yvette, France

[‡] Advanced Center for Bioorganic Chemistry of the Institute of Marine Biochemistry, Vietnam Academy of Science and Technology, 18 Hoang Quoc Viet, 8404, Cau Giay, Hanoi, Vietnam

ABSTRACT: Using a time-of-flight secondary ion mass spectrometer equipped with an argon cluster ion for sputtering and a bismuth liquid metal ion source for analysis, both surfaces of leaves and fruits of *Macaranga vedeliana*, an endemic New Caledonian species have been for the first time analyzed by a dual beam depth profiling. To prevent in-vacuum evaporation of the liquid content of the small glandular trichomes covering fruits and leaves surfaces, and also to be able to analyze their liquid content while preventing any sublimation of the latter, the samples were kept frozen during the whole experiment using a nitrogen cooled sample holder. Thus, it was possible to demonstrate that vedelianin, an active metabolite of the family of prenylated stilbenes named schweinfurthins, is only located in these glandular trichomes.

Depth profiling in organic materials remained for a very long time a challenge for time-of-flight secondary ion mass spectrometry (TOF-SIMS) instruments. While very efficient for surface analysis, monoatomic or cluster projectiles made of gold or bismuth^{1,2} were obviously not a good choice since these kinds of ion beams induce a large in-depth damage in organic layers due to a range of several tens of nanometers. A great hope arose, in the 2000s with the advent of C₆₀ fullerene ions sources,^{3,4} and a few years after with large argon cluster ion sources.⁵ These ion beams are made of a large number of atoms, each atom having itself a very low kinetic energy while the total kinetic energy of the entire cluster is in the range of a few tens of keV. The consequence is that these cluster ion beams are the most efficient to sputter surfaces layer after layer, particularly an organic sample, while the in-depth induced penetration of the individual constituents remains limited to a few Ångström, thus limiting the damage of the underlying layers. The relative advantages and drawbacks of these two ion sources, as well as the choice between single or dual beam depth profiling, are still under debate and need to be described, at least briefly. Several studies revealed that the fullerene projectiles were still causing some damage at the sample, thus with a subsequent decrease of the sputtering yield and a loss of depth resolution with sputtered depth.⁶ On the one side, C₆₀ or massive argon cluster ion beams can be used for both sputtering and analyzing the sample.^{7,8,9} In that case, while the analysis beam current is relatively limited, the reduction of the secondary ion fragmentation and the

increased sensitivity can be considered as important advantages, together with the use of only one single ion column. On the other side, bismuth cluster ion beams can be used for the analysis in conjunction with massive argon clusters for sputtering. This dual beam depth profiling method, while necessitating two different ion columns, offers the advantages of the very small focus and high current of the bismuth liquid metal ion guns, together with the flexibility offered by the large choice of the cluster size with an argon gas cluster ion source, from a few hundred up to several thousand argon atoms in a projectile. Proofs-of-concept of the feasibility of using any of these two methods for 3D-imaging and depth profiling in organic samples have already been published, with various samples like model layers,⁶ single cells,^{10,11} or animal tissue sections.¹²

Here the dual beam depth profiling method is used for the first time to detect and locate an active metabolite in small glandular trichomes which are found at the surface of leaves, inflorescences, bracts and fruits of *Macaranga vedeliana*, an endemic New Caledonian species. Glandular plant trichomes are epidermal outgrowths mainly found on the surface of leaves and stems of about 30 % of all vascular plants.¹³ They have a strong capacity to produce, store and secrete large quantities of secondary metabolites, which are an important first line of defense against herbivorous insects and pathogens.¹⁴ In some cases, glandular trichomes have been shown to function primarily as storage organs in fully developed leaves, with the produc-

tion of secondary metabolites at the onset of their development.¹⁵ In 2005, Guhling *et al.*¹⁶ showed that the prenylated flavanone nymphaeol-C was localized exclusively in glandular trichomes on the abaxial leaf side of *Macaranga tanarius*, a vietnamese species close to *M. vedeliana* that also produce vedelianin and other prenylated stilbene derivatives.¹⁷ Indeed, phytochemical studies from *Macaranga* species led to the discovery of an interesting family of prenylated stilbenes, named schweinfurthins (SWF), having an original hexahydroxanthene moiety. Vedelianin, the first member of this chemical series was isolated from the leaves of *Macaranga vedeliana*.¹⁸ Studying these molecules is of great interest since they display promising antiproliferative activities at low concentration (nM) for specific tumor-derived cell lines, such as glioblastoma.¹⁹ Currently, the study of these compounds is limited by supply problems. Indeed, the extraction yield is weak and only one total synthesis, requiring at least 16 steps with a poor overall yield, was achieved to date.²⁰

MATERIALS AND METHODS

Macaranga vedeliana samples

Bracts (small leaves which accompanies inflorescence) and fruits of *Macaranga vedeliana* (Baill.) Müll. Arg. were collected in April 2015 at Lifou, Luengoni, New Caledonia, authenticated by V. Dumontet (a voucher specimen [DUM-0716] has been deposited at the herbarium of the IRD center, New Caledonia), and immediately frozen *in situ*, in order to maintain intact the sample histology and composition, before being shipped, also frozen, to the mass spectrometry laboratory located in Gif-sur-Yvette, France. Small pieces of bracts and of the surface of fruits were cut, fixed onto 1 cm × 1 cm silicon wafers with the square frame of a sample holder specially designed by ION-TOF GmbH (Münster, Germany) to maintain the sample frozen under vacuum. The sample is in mechanical contact with a cold finger, which was itself kept cold by an external Dewar containing liquid nitrogen. A variable thermistor located in the sample holder is computer controlled thanks to a thermocouple measuring the temperature at the exact position of the small silicon wafer piece. The sample temperature chosen for all the experiments was -30 °C.

Figures 1a and 1b show fruit and fruit surface, and figures 1c and 1d bract and bract surface of *Macaranga vedeliana*. The small glandular vesicles (trichomes), which are clearly visible at the surface, have a size of 50-100 µm. Although both bracts and fruits were analyzed, the data were found to be very similar, thus leading to the same conclusions. Only the analyses of bracts are shown in the following.

Optical images of the analyzed areas of the samples were obtained with an Olympus BX51 microscope (Rungis, France), equipped with 1.25× to 50× lenses, a motorized scanning stage (Marzhauser Wetzlar GmbH, Wetzlar, Germany), a SC30 color camera, and monitored by the Olympus Stream Motion 1.9 software.

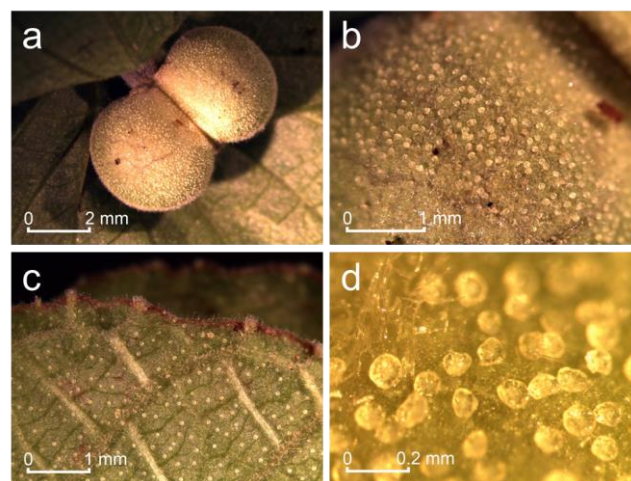


FIGURE 1: *Macaranga vedeliana* fruit and bract. a: fruit; b: fruit surface; c: lower face of the bract; d: lower face of the bract surface. Scale bars are indicated in each panel: a: 2 mm; b: 1 mm; c: 1 mm; d: 0.2 mm.

Vedelianin standard

10 µL of a vedelianin solution (1 mg.mL⁻¹ in methanol) (C₂₉H₃₆O₆, exact mass 480.2512 Da), of which the chemical structure is shown in Figure 2, were deposited onto a silicon wafer.

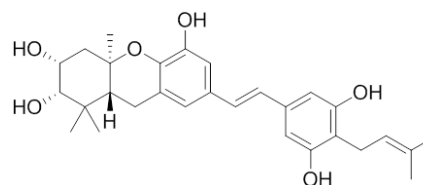


FIGURE 2: Chemical structure of vedelianin (C₂₉H₃₆O₆, exact mass 480.2512 Da), extracted from *Macaranga vedeliana*.

Dual beam depth profiling

The TOF-SIMS 2D- and 3D-imaging experiments were performed with a TOF-SIMS IV mass spectrometer (ION-TOF GmbH, Münster, Germany) located at the Institut de Chimie des Substances Naturelles (CNRS, Gif-sur-Yvette, France). This instrument is fitted with two types of ion sources, also manufactured by ION-TOF GmbH. One primary ion source is a liquid metal ion gun (LMIG) which delivers bismuth cluster ions (Bi₃⁺ selected with a 25 keV kinetic energy). This spectrometer is able to perform dual beam depth profiling, thanks to an argon cluster ion source. Ar_n⁺ ions (with n = 500 to 2000) with a kinetic energy between 5 and 20 keV hit the sample surface with an angle of incidence of 45°. The emitted secondary ions were accelerated to a kinetic energy of 2 keV (2 kV extraction) toward a field-free region and a single-stage reflectron (first-order compensation). Secondary ions were post-accelerated to a kinetic energy of 10 keV before hitting the detector composed of a micro-channel plate, a scintillator and a photomultiplier. Between two primary ion pulses, a low energy (~20 eV) electron flood gun was used to neutralize the sample surface. Pulsed primary ion currents were measured with a Faraday cup located on the grounded sample holder. Two modes of

focusing the bismuth primary ions were used. With the first focusing mode, which is named “high current bunched mode” (HCBU), the beam diameter was 2–5 μm , while for the second one, which is named “burst alignment plus delayed extraction” (BA-DE), the diameter of the beam was 400 nm. With the HCBU mode the primary ion pulses were bunched so that their duration of $\sim\text{ns}$ enabled a mass resolution of ~ 3000 ($M/\Delta M$, FWHM, at m/z 400). With the BA-DE mode the primary ion pulses were not bunched but the extraction of the secondary ions was delayed so that a mass resolution of ~ 8000 could be reached. A detailed description and comparison of these two modes of acquisition can be found elsewhere.²¹

Positive and negative ion images were recorded with the following parameters (only positive ion images are shown):

Analysis of vedelianin standard: Mass spectrum recorded in HCBU mode over an area of $500\ \mu\text{m} \times 500\ \mu\text{m}$, with 128×128 pixels and a Bi_3^+ primary ion dose (PID) of 1.4×10^{10} ions/ cm^2 .

2D-imaging: Secondary ion images were recorded in BA-DE mode over an area of $400\ \mu\text{m} \times 400\ \mu\text{m}$, pixel size $400\ \text{nm} \times 400\ \text{nm}$, 1024×1024 pixels, analysis dose 2.0×10^{11} ions/ cm^2 .

3D-imaging: Irradiation with a 20 keV energy Ar_{1400}^+ sputtering beam, with a current of 10 nA, over an area of $700\ \mu\text{m} \times 700\ \mu\text{m}$ (the Ar_n^+ beam size is $\sim 50\ \mu\text{m}$ wide, with a Gaussian-like profile), followed by a surface analysis with Bi_3^+ primary ions in HCBU mode over an area of $500\ \mu\text{m} \times 500\ \mu\text{m}$ inside and at the center of the previously sputtered area. Analysis pixel size $2\ \mu\text{m} \times 2\ \mu\text{m}$, 256×256 pixels, analysis dose per each analysis scan 1.5×10^{11} ions/ cm^2 , sputter beam dose per each scan 9.3×10^{13} ions/ cm^2 , 430 scans, total analysis time 24.5 h, total analysis and sputtering doses 6.3×10^{13} and 4.0×10^{16} ions/ cm^2 , respectively.

The internal mass calibration was performed using low mass ions always present: H^+ , C^+ , CH^+ , CH_2^+ , CH_3^+ , CH_4^+ , C_2H_3^+ and C_2H_5^+ in the positive ion mode and H^- , C^- , CH^- , C_2^- , C_3^- , and C_4H^- in the negative ion mode.

In the ion images, the maximum number of counts MC corresponds to the amplitude of the color scale [0,MC], and TC is the total number of counts recorded for the specified m/z (it is the sum of counts in all the pixels).

RESULTS AND DISCUSSION

Analysis of vedelianin standard

Figure 3 shows parts of positive ion mass spectra of a pure vedelianin compound and of the *Macaranga vedeliana* sample during the 3D-imaging analysis. With the pure compound the positive $[\text{M}]^+$ ion of vedelianin is detected at m/z 480.275, and in the biological sample at m/z 480.227, respectively, while the calculated value is m/z 480.2512. The standard deviations are +50 and -50 ppm, respectively, which are acceptable mass accuracies during the TOF-SIMS on tissue analysis of organic compounds.

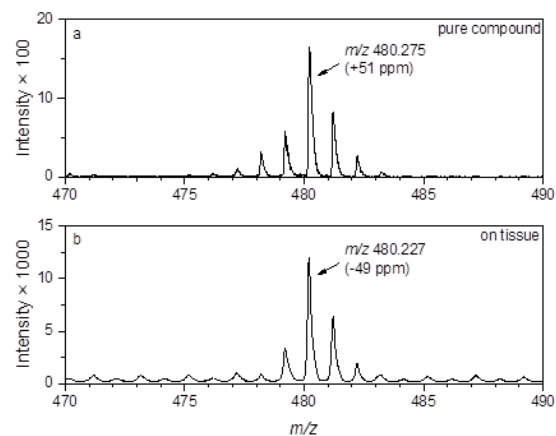


FIGURE 3: Parts of positive ion TOF-SIMS mass spectra showing the detection of the $[\text{M}]^+$ ion of vedelianin (calculated m/z 480.2506). a: recorded from a pure compound; b: extracted from the 3D-imaging experiment.

Surface analysis of a *Macaranga vedeliana* bract at room temperature

Figure 4 shows ion images recorded at the surface of a bract. During this first analysis, the sample was defrosted under vacuum before the analysis, and further analyzed at room temperature using the so-called BA-DE mode.²¹ A glandular trichome is clearly seen in the total ion image (Figure 4a), which shows very nicely the histology of the bract surface. However, the trichome appears as being flattened out, as if all the liquid contained in it has disappeared.

Then an ion image (Figure 4b) is generated by the selection of a window in the mass spectrum around the mass-to-charge value of vedelianin (± 0.2 Da, similar to the base peak width in Figure 3). In this ion image vedelianin is not found to be located in the glandular trichome, but rather diffuse and not precisely localized. A precise examination of the corresponding peak in the mass spectrum shows a standard deviation of more than -250 ppm and above all an isotopic distribution which does not fit the one of the pure compound analyzed previously. This indicates that the peak selected at the m/z value of vedelianin does not correspond to this compound but to something else, like a surface contamination or noise. This first experiment shows that vedelianin cannot be detected under these experimental conditions, because the bismuth cluster ion beam does not go through the trichome membrane, or because vedelianin has evaporated under vacuum, as suggested by the flattened form of the trichome.

The same experiment was repeated but with a sample kept frozen under vacuum. Vedelianin was not detected, neither at the surface of the trichome, nor elsewhere at the surface of the bract. Finally, it was also tried to cut the trichome membrane with a scalpel, while always keeping the sample frozen. Then vedelianin was finally detected, mostly around the trichome. All these surface analyses indicate that vedelianin is not present at the surface of

the bract, nor at the surface of the trichomes, but likely within the latter. A 3D analysis by dual beam depth profiling is necessary to validate this hypothesis.

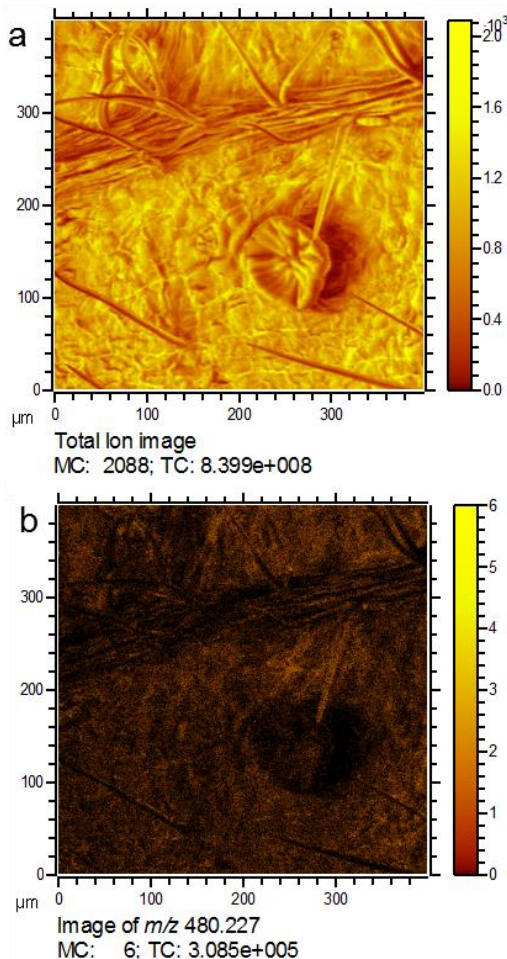


FIGURE 4: 2D-ion images of the surface of a *Macaranga vedeliana* bract. a: Total ion image; b: image of a mass selection at m/z 480.227 corresponding to the expected $[\text{M}]^+$ ion of vedelianin. Image size $400 \mu\text{m} \times 400 \mu\text{m}$, 1024×1024 pixels, pixel size $400 \text{nm} \times 400 \text{nm}$.

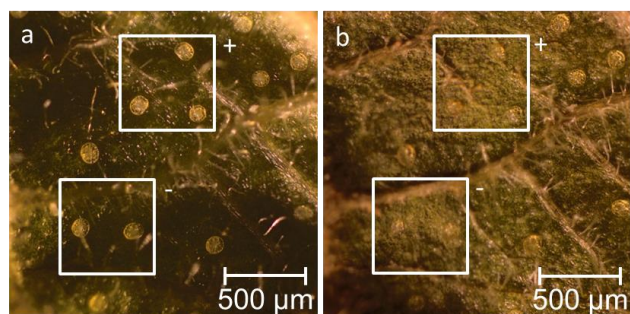


FIGURE 5: Images of a *Macaranga vedeliana* bract before and after the dual beam depth profiling analysis. a: before the analysis; b: after the analysis. White squares ($500 \mu\text{m} \times 500 \mu\text{m}$) indicate the analyzed areas, in positive ion mode (+) and negative ion mode (-), respectively. Scale bars: $500 \mu\text{m}$.

Dual beam depth profiling of a frozen *Macaranga vedeliana* bract

Figure 5 shows pictures of a frozen *Macaranga vedeliana* bract before and after the dual beam depth profiling. Two areas, labeled "+" and "-", were chosen, with several trichomes in each, for a positive and a negative ion modes analyses, respectively. While the trichomes can be easily observed before the analysis in Figure 5a, these structures are almost unobservable after the sputtering of the sample with the $20 \text{keV Ar}_{1400}^+$ irradiation, indicating that it has been entirely sputtered. On the contrary, some trichomes remain clearly observable outside of the sputtered area, like those at the upper right corner of the images of Figure 5. This indicates that the disappearance of the trichomes in the sputtered area is not due to any in-vacuum evaporation, but is really a consequence of the argon cluster sputtering.

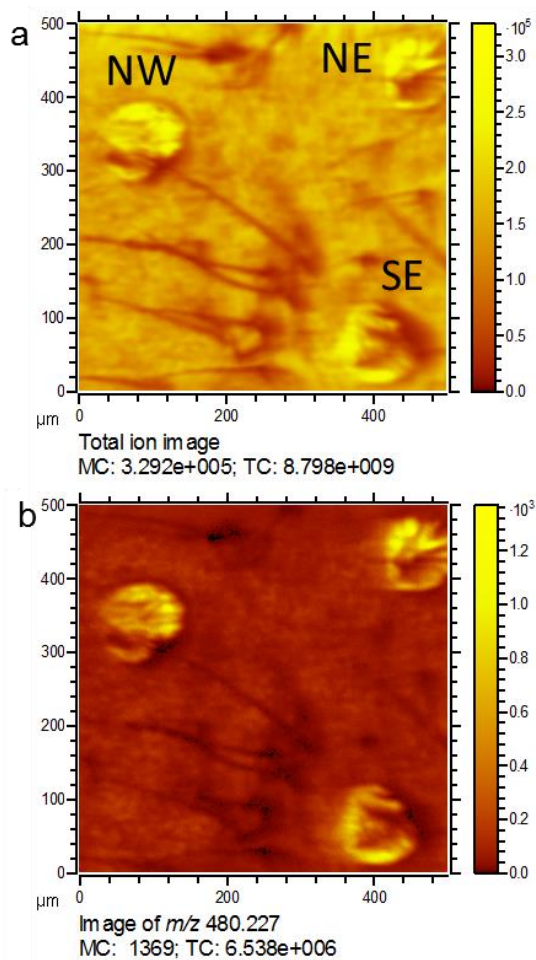


FIGURE 6: 2D-ion images (positive ion mode) extracted from the dual beam depth profiling of a *Macaranga vedeliana* bract. a: Total ion image; b: Image of the m/z 480.227 $[\text{M}]^+$ ion of vedelianin. The three trichomes detected in the ion image are labeled NW, NE, and SE. Image size $500 \mu\text{m} \times 500 \mu\text{m}$, 256×256 pixels, pixel size $2 \mu\text{m} \times 2 \mu\text{m}$.

Figure 6a shows the total ion image reconstructed from the sum of all the analysis data during the dual beam depth profiling. Since this ion image was recorded in the

HCBU mode, and a pixel size of $2\ \mu\text{m} \times 2\ \mu\text{m}$ only, the histology of the sample is obviously not as well represented as in the total ion image in Figure 4a. This analysis mode was chosen in that case to maintain a maximum acquisition time of 24 hours. Nevertheless the anatomical structures of the bract are easily observable, particularly the three trichomes, which are detected with a larger total ion intensity than in the other parts of the image. These three trichomes are labeled, according to their localization in the image, NW (North-West), NE (North-East), and SE (South-East), respectively. Figure 6b shows the ion image of $m/z\ 480.227\ [\text{M}]^+$ ion of vedelianin. This figure clearly demonstrates that vedelianin is now detected in the trichomes during the dual beam depth profiling. Figure 7 shows the 3D volume reconstruction of the intensity of the $m/z\ 480.227\ [\text{M}]^+$ ion of vedelianin, with an arbitrary z-scale proportional to the number of scans or to the Argon cluster fluence. Figure 8 shows the intensity of the same ion, as a function of the Ar cluster fluence, and in three regions of interest (ROI) drawn around the NW, SE, and NE trichomes, as labeled in Figure 6a. These two figures show that vedelianin is not detected at the beginning of the profile (below 0.4×10^{16} ions/cm²), while the intensity dramatically increases after. The 3D reconstruction and the intensity profiles show that vedelianin is detected in the trichomes, not elsewhere, after having sputtered the trichome membrane.

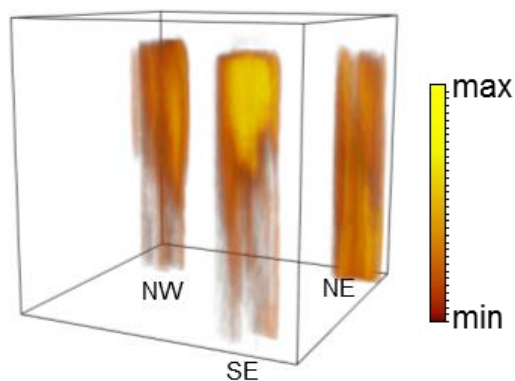


FIGURE 7: 3D volume reconstruction extracted from the dual beam depth profiling of a *Macaranga vedeliana* bract showing the intensity of the $m/z\ 480.227\ [\text{M}]^+$ ion of vedelianin. x and y scales 500 μm , arbitrary z scale.

For the NW and SE trichomes, the intensity of the vedelianin ion decreases at the end of the depth profiling, with an argon cluster fluence of 4.0×10^{16} ions/cm², down to values larger than at the beginning but much smaller than the maxima. This shows that these two trichomes are quite entirely sputtered. Figures 7 and 8c also show that the intensity of the trichome labeled NE does not decrease, which indicates that the latter is not entirely sputtered. This is in agreement with Figure 5b, where it is observed that the NE-trichome is the only one which is still somewhat visible after the depth profiling.

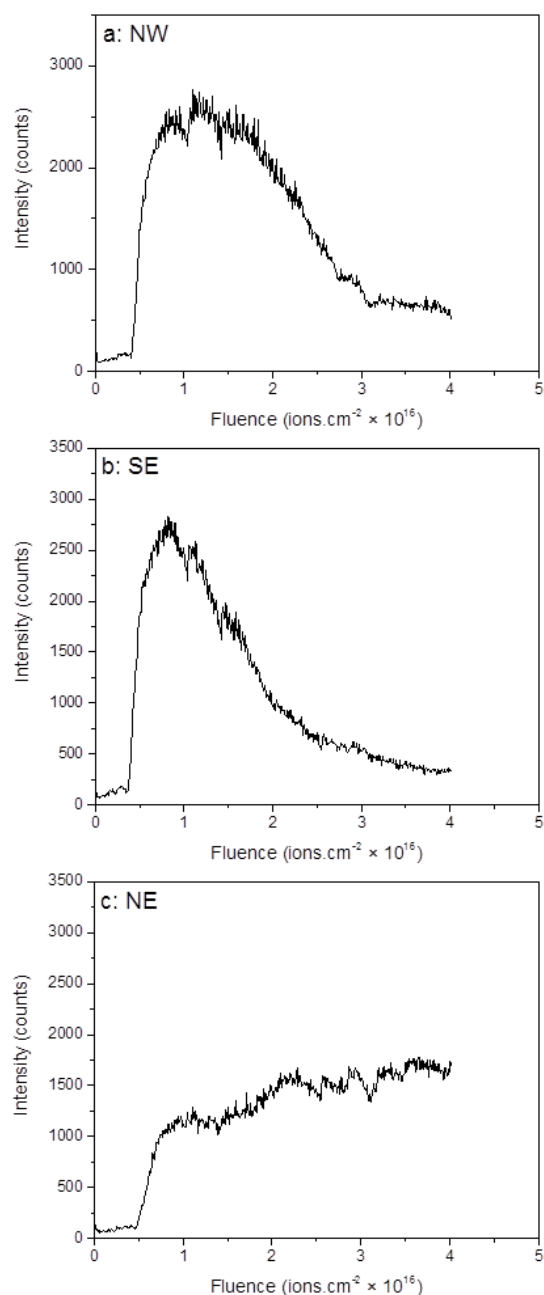


FIGURE 8: Intensity of the $m/z\ 480.227\ [\text{M}]^+$ ion of vedelianin as a function of the fluence of Ar_{1400}^+ sputtering ions, in the trichomes (selected by ROI) of NW, SE, and NE trichomes as defined in Figure 6a. a: NW trichome; b: SE trichome; c: NE trichome.

CONCLUSION

Using TOF-SIMS dual beam depth profiling with argon and bismuth clusters, it has been for the first time possible to precisely detect and locate an active metabolite in glandular trichomes lying at the surface of leaves and fruits from a New Caledonian plant. To achieve this result, it was necessary to keep the sample frozen during the acquisition, in order to avoid any evaporation or delocalization of the liquid compound. This new kind of 3D analysis opens the way to precise localization of metabolites in plants, without chemical fixation, which would

change the composition or hide a part of the chemical content of the sample. In the present case of *Macaranga vedeliana*, the study of metabolites is limited by supply problems, because of weak extraction yield or long total synthesis with a poor overall yield. Thus, in order to possibly be able to improve the extraction yield, a precise knowledge of the place of storage or production of the compounds in the plant is of the greatest interest.

AUTHOR INFORMATION

Corresponding Author

* Phone: +33 169 824 575. E-mail: Alain.Brunelle@cnrs.fr

ORCID

Nicolas Elie: [0000-0002-8733-0971](https://orcid.org/0000-0002-8733-0971)

David Touboul: [0000-0003-2751-774X](https://orcid.org/0000-0003-2751-774X)

Fanny Roussi: [0000-0002-5941-9901](https://orcid.org/0000-0002-5941-9901)

Marc Litaudon: [0000-0002-0877-8234](https://orcid.org/0000-0002-0877-8234)

Alain Brunelle: [0000-0001-6526-6481](https://orcid.org/0000-0001-6526-6481)

Author Contributions

#These authors contributed equally.

ACKNOWLEDGMENT

This work was supported by the Agence Nationale de la Recherche (grant ANR-2015-CE29-0007-01 DEFIMAGE), and has benefited from an “Investissement d’Avenir” grant managed by Agence Nationale de la Recherche (CEBA, ref. ANR-10-LABX-25-01). T.P. is also grateful to the doctoral school “Innovation thérapeutique du fondamental à l’appliqué” from Paris-Saclay University for a PhD research fellowship. The authors are grateful to Loyalty Island Province of New Caledonia, which facilitated the field investigation.

REFERENCES

- (1) Davis, N.; Weibel, D.E.; Blenkinsopp, P.; Lockyer, N.; Hill, R.; Vickerman, J.C. *Appl. Surf. Sci.* **2003**, *203-204*, 223-227.
- (2) Touboul, D.; Kollmer, F.; Niehuis, E.; Brunelle, A.; Laprévotte, O. *J. Am. Soc. Mass Spectrom.* **2005**, *16*, 1608-1618.
- (3) Weibel, D.; Wong, S.; Lockyer, N.; Blenkinsopp, P.; Hill, R.; Vickerman, J.C. *Anal. Chem.* **2003**, *75*, 1754-1764.
- (4) Debois, D.; Brunelle, A.; Laprévotte, O. *Int. J. Mass Spectrom.* **2007**, *260*, 115-120.
- (5) Matsuo, J.; Okubo, C.; Seki, T.; Aoki, T.; Toyoda, N.; Yamada, I. *Nucl. Instrum. Methods Phys. Res. B*, **2004**, *219-220*, 463-467.
- (6) Shard, A.G.; Havelund, R.; Seah, M.P.; Spencer, S.J.; Gilmore, I.S.; Winograd, N.; Mao, D.; Miyayama, T.; Niehuis, E.; Rading, D.; Moellers R. *Anal. Chem.* **2012**, *84*, 7865-7873.
- (7) Winograd, N. *Surf. Interface Anal.* **2013**, *45*, 3-8.
- (8) Fletcher, J.S.; Rabbani, S.; Henderson, A.; Lockyer, N.P.; Vickerman, J.C. *Rapid Commun. Mass Spectrom.* **2011**, *25*, 925-932.
- (9) Fletcher, J.S. *Biointerphases* **2015**, *10*, 018902-1-8.
- (10) Passarelli, M.K.; Newman, C.F.; Marshall, P.S.; West, A.; Gilmore, I.S.; Bunch, J.; Alexander, M.R.; Dollery, C.T. *Anal. Chem.* **2015**, *87*, 6696-6702.
- (11) Vanbellingen, Q.P.; Castellanos, A.; Rodriguez-Silva, M.; Paudel, I.; Chambers, J.W.; Fernandez-Lima, F.A. *J. Am. Soc. Mass Spectrom.* **2016**, *27*, 2033-2040.
- (12) Bich, C.; Havelund, R.; Moellers, R.; Touboul, D.; Kollmer, F.; Niehuis, E.; Gilmore, I.S.; Brunelle, A. *Anal. Chem.* **2013**, *85*, 7745-7752.
- (13) Glas, J.J.; Schimmel B.C.J.; Alba, J.M.; Escobar-Bravo, R.; Schuurink, R.C. *Int. J. Mol. Sci.* **2012**, *13*, 17077-17103.
- (14) Fahn, A. In *Plant Trichomes*; Hallahan, D.L.; Gray, J.C. Eds.; Academic Press, New York, NY, USA, 2000; pp 37-45.
- (15) Valkama, E.; Salminen, J.P.; Koricheva, J.; Pihlaja, K. *Ann. Bot.*, **2004**, *94*, 233-242.
- (16) Guhling, O.; Kinzler, C.; Dreyer, M.; Bringmann, G.; Jetter, R. *J. Chem. Ecol.* **2005**, *31*, 2323-2341.
- (17) Allard, P.M.; Péresse, T.; Bisson, J.; Gindro, K.; Marcourt, L.; Pham, V.C.; Roussi, F.; Litaudon, M.; Wolfender, J.L. *Anal. Chem.* **2016**, *88*, 3317-3323.
- (18) Thoison, O.; Hnawia, E.; Guéritte-Voegelein, F.; Sévenet, T. *Phytochemistry* **1992**, *31*, 1439-1442.
- (19) Beutler, J.A.; Shoemaker, R.H.; Johnson, T.; Boyd, M.R. *J. Nat. Prod.* **1998**, *61*, 1509-1512.
- (20) Topczewski, J.J.; Neighbors J.D.; Wiemer, D.F. *J. Org. Chem.* **2009**, *74*, 6965-72.
- (21) Vanbellingen, Q.P.; Elie, N.; Eller, M.J.; Della-Negra, S.; Touboul, D.; Brunelle, A. *Rapid Commun. Mass Spectrom.* **2015**, *29*, 1187-1195.



For TOC only
